RSC Advances

PAPER

View Article Online
View Journal | View Issue

Cite this: *RSC Adv.*, 2026, **16**, 8533

Synthesis of isoxazoles and their hydrazinolysis to 5-aminopyrazoles: an approach to fluorescent derivatives

María-Camila Ríos, Alexander Ladino-Bejarano, Gian Pietro Miscione and Jaime Portilla *

A protocol for the synthesis of 5-arylisoxazoles and their TFA-mediated hydrazinolysis to 5-amino-3-aryl-1*H*-pyrazoles was developed using readily available ketones as starting materials and eco-friendly microwave-assisted conditions. All reactions proceeded in high yields, and although some of the obtained heteroamines are commercially available, they are challenging to obtain because they are expensive or require access to equally expensive substrates. A computational study using TD-DFT calculations was conducted to better understand the reaction mechanism of the isoxazole ring-opening reaction with hydrazine in water. Ultimately, the photophysical properties of some fluorescent products were conveniently explored.

Received 4th December 2025
Accepted 4th February 2026

DOI: 10.1039/d5ra09395c

rsc.li/rsc-advances

Introduction

Pyrazole and isoxazole derivatives are an essential family of five-membered aza-heterocyclic compounds (AHCs) with pertinent applications in biological (medicinal, agrochemical, *etc.*), physical (materials science, optoelectronics, *etc.*), industrial (drugs, dyes, explosives, *etc.*), and synthetic fields.[1–6] These 1,2-azoles are frequently obtained by cyclocondensation reactions of 1,3-bis-electrophiles with hydrazines or hydroxylamine, respectively, although at times, [3 + 2] cycloadditions have been used to access them.[3,7,8] They are key intermediates to access more complex structures with better properties,[5,9,10] and numerous derivatives have been used as anti-inflammatory, anti-cancer, antibiotic, and antifungal drugs, among others.[11–18] They have also been found in fluorescent molecules[19–21] and energetic materials[7,22,23] (Fig. 1).

Pyrazoles have shown greater synthetic weight than isoxazoles because of the higher reactivity of the π-excessive pyrazole ring compared to the one with the oxygen atom.[1–5,7] In this respect, 5-aminopyrazoles are important as 1,3-bis-nucleophilic reagents in obtaining 5:6 aza-fused motifs (*e.g.*, pyrazolo[3,4-*b*]pyridines[24] and pyrazolo[1,5-*a*]pyrimidines[6]) by their reaction with 1,3-bis-electrophiles, which are biologically and photophysically relevant AHCs.[6,24,25] These amines are obtained by reacting hydrazines with acrylonitriles bearing an easily movable group at the Cβ (*e.g.*, β-enaminonitriles or enolizable β-ketonitriles) to yield the aromatic ring substituted with an amino group.[7] For example, 5-amino-NH-pyrazoles are obtained from hydrazine monohydrate (HM). The acrylonitrile derivatives usually used (*i.e.*, X = NH_2, OH, or Cl) are reactive substrates that exhibit synthetic (several-stage reactions), storage, and handling difficulties[7] (Scheme 1a and 1b).

Although most reported syntheses of 5-aminopyrazoles use toxic, hazardous, or flammable reagents (*e.g.*, $POCl_3$ in the synthesis of β-chloroacrylonitriles),[7,26] their access *via* acrylonitriles remains the usual method.[7] Thus, there is a need for efficient protocols that use easy-to-handle substrates. In 1941, Bell[27] reported the hydrazinolysis of 5-methylisoxazole to form 5-amino-3-methyl-*N*-arylpyrazoles, *in situ* generating acetylacetonitrile; however, this method has been poorly studied due to limited access to diverse isoxazoles.[28,29] In 2016, Kallman *et al.*[30] reported a similar route to yield 5-amino-3-aryl-1*H*-pyrazoles **4** from 5-arylisoxazoles **3** and HM under basic conditions in one or two reaction stages (Scheme 1b); they followed up the reaction by NMR to establish the optimal conditions and the mechanism. Although this report is from almost a decade ago, this pyrazole type is still obtained from acrylonitriles,[1,2,7] and

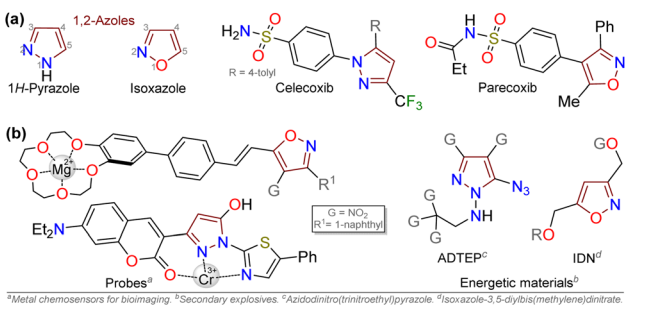

Fig. 1 Pyrazoles and isoxazoles of (a) biological and (b) physical interest.

Department of Chemistry, Universidad de Los Andes, Carrera 1 No. 18A-10, Bogotá 111711, Colombia. E-mail: jportill@uniandes.edu.co

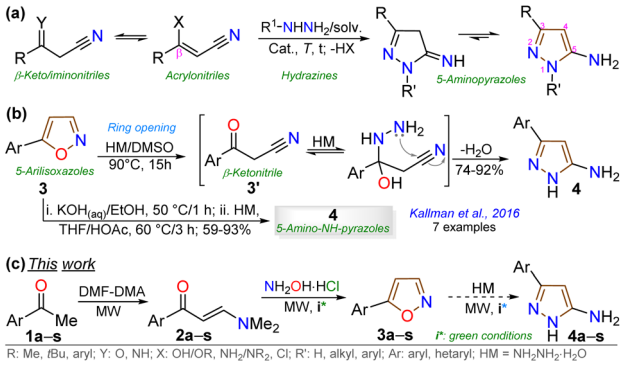

Scheme 1 Synthesis of 3-substituted 5-aminopyrazoles using (a) acrylonitriles (*via* classical cyclocondensation) or (b and c) 5-arylisoxazoles (*via* opening ring).

protocols based on isoxazoles are rare,[31–34] or are found in patents of diverse complex products.[35,36] These results match the reduced substrates disposal or the reaction's scope, thereby limiting later transformations.[30–36]

The cited protocols have some operational shortcomings, such as poor to moderate yields and long reaction times (up to 2 days), requiring several reaction steps with solvents that can be difficult to remove and could originate contamination. Likewise, most of these methods require an excess of acid (HCl, HOAc, *etc.*) or base (KOH, MeONa, *etc.*), or even protective groups.[30–36] Recently, our group synthesized and photophysically studied four fluorescent isoxazoles substituted with 1-pyrenyl (**3n**) and 3-coumarinyl (**3o–q**) rings (Scheme 2), which exhibited notable acidochromism in trifluoroacetic acid (TFA) *via* an intramolecular charge-transfer (ICT) process.[20,37] This process is maybe the most relevant among molecular optical mechanisms, with several examples involving AHCs with diverse donor–acceptor molecular architecture.[20,38–41] Dyes **3n–q** were obtained by the microwave-assisted reaction of hydroxylamine hydrochloride (HH) with β-enaminones **2n–q**; this substrate type has proved to be convenient to access isoxazoles **3**,[20,37,42] and other AHCs, and our group has developed numerous syntheses with them.[20,37,43,44] Therefore, we aim to optimize the hydrazinolysis of a 5-arylisoxazole derivative to the respective 5-amino-NH-pyrazole under microwave (MW) conditions; then to obtain a broad family of isoxazoles **3a–s** and evaluate their hydrazinolysis reaction to 5-aminopyrazoles **4a–s** (Scheme 1c).

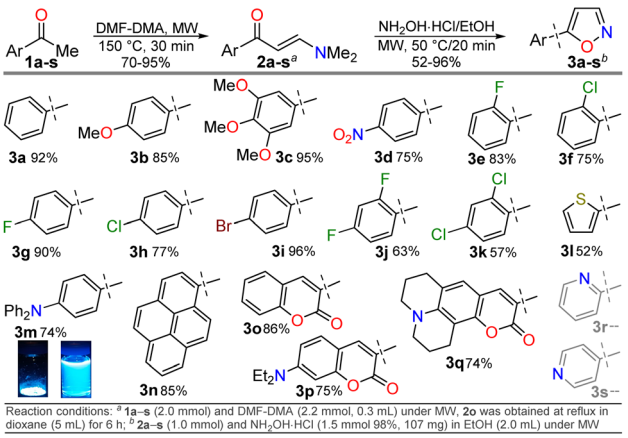

Scheme 2 Synthesis of β-enaminones **2a–s** and isoxazoles **3a–q**.

Results and discussion

Synthesis

We initiated the study by exploring a standard synthetic route to a family of 5-(hetero)arylisoxazoles under mild and eco-friendly conditions. First, β-enaminones **2a–s** were obtained by a MW-assisted method, which is widely used in our laboratory[20,37,43,44] or adapting other reported methodologies,[45,46] see SI for details; β-enaminones **2a–s** contain diverse (hetero)aryl groups and were obtained in high yields (70–95%). Then, the synthesis of isoxazoles **3a–s** was explored by MW-assisted reactions of **2a–s** with HH.[30,47] This reaction was conducted in the absence of base to favor the 5-aryl regioisomer over the 3-aryl regioisomer obtained in basic media; this result is due to the nitrogen atom's lower nucleophilicity in acidic media, which favors initial attack by the oxygen atom on the carbonyl group.[30,47] Such as **2a–s** or the reported isoxazoles **3n–q**,[20,37] the electronic nature of substituents does not govern the reaction yields of **3a–q** (52–96%). However, reactions do not occur with pyridyl-substituted reagents **2r** and **2s**, even under variable conditions (temperature, time, solvent, *etc.*), although **3r** and **3s** were previously reported.[48] We assume the reaction does not proceed due to the poor solubility of precursors in the presence of HCl (from HH), as minimal solvent is used in the MW tubes and salts are formed; however, **3r** and **3s** could not be obtained under reflux[48] so this report should be revised. Notably, the triphenylamine derivative **3m** exhibited a higher fluorescence in both solution and the solid state than isoxazole **3n–q**; thus, its photophysics are described in the last section (Scheme 2).

Subsequently, we envisaged that the MW-assisted hydrazinolysis reaction of **3a–q** with HM could yield 5-amino-1*H*-pyrazoles **4a–q**, given the proven advantages of the MW synthesis[20,37,43,44] and difficulties shown by the cited methods.[30–36] Thus, we aimed to optimize a protocol using the model substrate **3h** and varying solvent, time, temperature, and the presence of an additive (Table 1). The first experiments were performed under conditions described by Kallman *et al.*,[30] but under microwaves for 1 hour (Entries 1–3), offering very low reaction yields without significant consumption of the substrate. We then use other polar solvents, including EtOH, MeOH, and H_2O, and even in the absence of any solvent at high temperatures (Entries 4 to 11), finding an increase in reaction yield, but without exceeding 50%. We observed higher yields when the reaction was carried out at 150 °C for 15 minutes; thus, the reaction was continued under these conditions.

In the study of improving yields in eco-friendly conditions, it was decided to carry out the reaction in water and in the presence of an additive, finding that decomposition products with **4h** were generated in the presence of strong acids/bases, which did not allow proper isolation of the product (Entries 12 to 14). Finally, the reaction markedly improved when TFA was used

Table 1 Optimization for the synthesis of the 5-amino-NH-pyrazole 6a [a]

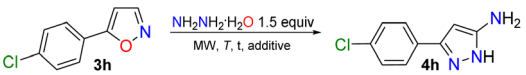

Entry	Solvent	Additive (equiv.)	T (°C)	t (min)	Yield. (%)
1			90	60	7
2	DMSO		120	60	12
3			150	60	13
4	EtOH		120	20	NA[b]
5			150	20	34
6	ACN	Absence	120	20	18
7			150	20	40
8	Absence		150	20	50
9			120	20	35
10			150	20	46
11			150	15	47
12	H_2O	NaOH (0.1–1)	150	15	
13		HCl (0.1–1)	150	15	DP[c]
14		H_2SO_4 (0.1–1)	150	15	
15		TFA (0.1–1)	150	15	~95
16[d]		TFA (0.1)	Reflux	1440	10

[a] Reaction conditions: 3 h (0.25 mmol, 44.9 mg) and HM (1.5 equiv, 19 μL) under MW. [b] NA: Reaction does not advance. [c] DP: Decomposition product. [d] Under conventional heating.

(Entry 15), possibly due to its proven excellent interaction with the isoxazole rings.[20,37] Thus, the optimal conditions for yielding **4h** are those of entry 15: microwave irradiation in water with TFA as a catalyst at 150 °C for 15 minutes. Notably, the former product precipitates under these reaction conditions and can be recovered with good purity by simple filtration and washing (see SI for details).

Once the optimal conditions for obtaining **4h** were established, the scope of this synthesis was studied (Scheme 3). Initially, the introduction of diverse aryl groups and a π-excessive 2-thienyl ring was evaluated using substrates **3a–l.** Unfortunately,

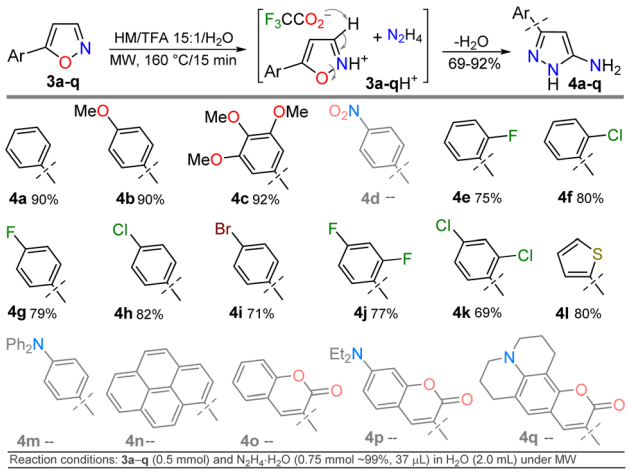

Scheme 3 Synthesis of 5-amino-3-aryl-NH-pyrazoles **4a–o**.

it was not possible to obtain the nitro-derivative **4d** due to the poor solubility in water of the substrate; possibly, the strong extractive nature of the nitro group into **3d** disfavors the initial protonation of the azole nitrogen[20,37] to solubilize it and start the reaction. By introducing fluorophoric groups in substrates (*i.e.*, TPA in **3m**, 1-pyrenyl in **3n**, or 3-coumarinyl in **3o–q**) to obtain new pyrazoles useful in fluorophore discovery, none of the expected products were obtained; these results are possibly due to stereoelectronic factors, solubility in water,[20,37] or decomposition (*e.g.*, hydrolysis) of the coumarin ring under the optimized reaction conditions. Thus, this reaction does not work with isoxazoles bearing strongly electron-donor or electron-acceptor groups, as they reduce the substrate's electrophilicity or basicity, respectively. For example, the nucleophilic attack of hydrazine on **4m** does not occur, nor does the protonation of **4d** to favor its solubility in water.

The obtained compounds (substituted β-enaminones **2a–s**, 5-(hetero)arylisoxazoles **3a–q**, and 5-aminopyrazoles **4a–c** and **4e–l**) were characterized by NMR spectroscopy and high-resolution mass spectrometry (HRMS). Notably, not all quaternary carbon atoms for the 5-(2-haloaryl)isoxazoles **4e,f** and **4j,k** could be observed *via* ^{13}C NMR spectra due to their multiple conformers and tautomers in equilibrium (see SI for details, Fig. S3–S41).

Computational DFT study

To gain deeper insight into the reaction mechanism of the TFA-catalyzed synthesis of 5-aminopyrazoles **4a–l**, we investigated the pathway leading to **4h** using density functional theory (DFT) simulations. These ground-state calculations were performed with the Gaussian 16,[49] software package at the M08-HX/6-311G* level of theory. The M08-HX functional[50] was chosen for its high accuracy in describing reaction mechanisms, barrier heights, proton-transfer processes, and non-bonding interactions, which characterize this process.[51–53] The 6-311G* basis set provides a balanced and well-established compromise between accuracy and computational cost for geometry optimizations and barrier heights. To represent the experimental environment, an implicit solvation model based on density (SMD) was used in water. The theory set used has proven to offer exceptional results in other mechanisms studied by us[44,54] (Fig. S49; see SI for more details).

Considering the pK_a values of reagents, an aqueous acid–base equilibrium with the respective conjugated species (*i.e.*, CF_3COO^- and $N_2H_5^+$) can be given (see SI for details). In addition, the special interaction of the isoxazole ring with an acid medium (*i.e.*, TFA),[20,37] could favor the substrate solubility. Thus, as the asymptotic limit (reactant energy) of the reaction profile, the reactive complex **R** was studied; this complex has a molecule of **3h**, a trifluoroacetate anion (AO^-), and a hydrazinium cation (MHH^+); a water molecule can be included in the entire mechanism to explain the process (Schemes 4, 5 and S1).

The complete mechanism for the formation of **4h** is described in the SI, and the essential steps are detailed below (Scheme 5). The first stage involves isoxazole ring opening at the transition state **TS1** (40.7 kcal mol^{-1}), which is the reaction-

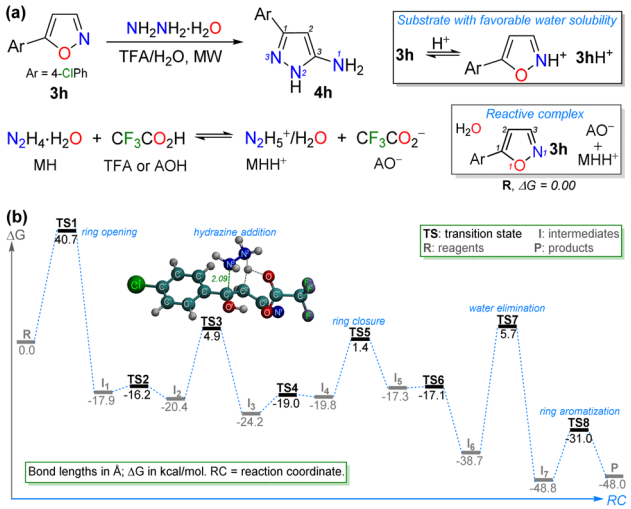

Scheme 4 (a) Mechanistic considerations and (b) energetic profile for the TFA-mediated formation of the 5-aminopyrazole **4h** in water.

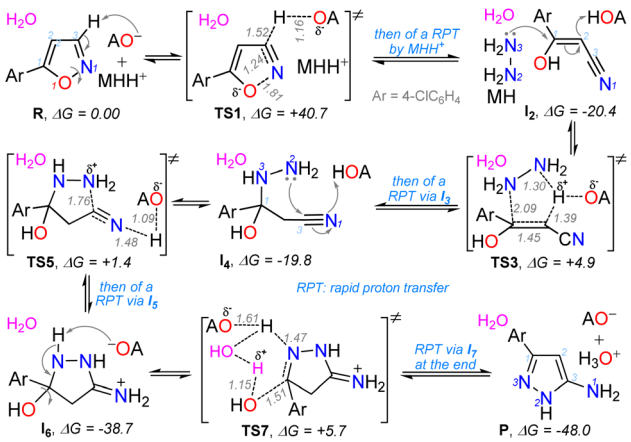

Scheme 5 Essential steps of the proposal mechanism for the formation of **4h**.

determining step, followed *via* a rapid proton transfer to yield the acrylonitrile intermediate $\mathbf{I_2}$. The high energy of **TS1** is consistent with the experimental results, as an elevated temperature (160 °C) was required for the reaction; however, it should be noted that the short reaction time observed (15 min) is characteristic of MW-assisted reactions.[20,37,43,44] The latter relevant step produces the cyclization intermediate $\mathbf{I_4}$ upon conjugated hydrazine addition to $\mathbf{I_2}$ *via* **TS3** (4.9 kcal mol^{-1}), followed by a second rapid proton transfer (RPT). In the third key step, the cyclization of $\mathbf{I_4}$ forms the new ring in $\mathbf{I_6}$ (highly stable, −38.7 kcal mol^{-1}) *via* the transition state **TS5** (1.4 kcal mol^{-1}) and a third RPT (Schemes 4b and 5). Finally, the removal of a water molecule in $\mathbf{I_6}$ through **TS7** (5.7 kcal mol^{-1}) and a fourth rapid proton transfer allows the system to evolve into the final pyrazole structure in **P** with aromaticity restored, now 48.0 kcal mol^{-1} more stable than the reactive complex (Schemes 4b, 5 and S1; see SI for more detail).

Photophysical results

Recently, we have established that the four isoxazoles **3n–q** (1-pyrenyl and 3-coumarinyl derivatives) are fluorescent molecules with noticeable photophysical properties in both solution and the solid state.[20,37] Here, we obtained the TPA derivative **3m**, studied its photophysics, and compared the results with those of **3n–q** and the standard Prodan, discovering that **3m** exhibits the best properties. The absorption and emission spectra of the six dyes were measured in 12 solvents of varying polarity at ~20 °C and 27 μM (Table 2). No significant changes in the absorption maxima were observed as solvent polarity increased for all dyes (Table S22 and Fig. S42a); however, by averaging the values obtained for the absorptivity coefficient (ε) of isoxazoles **3m–q**, we found that they showed higher ε values than Prodan. Notably, the ε value increases with the electron-donor nature of the fluorophoric ring in the dye due to improved intramolecular charge transfer (ICT) phenomena from such donor groups towards the nitrogen atom of the isoxazole ring, π-deficient in character. In addition, this ICT process favors the π-extended system, which offers improved ε values[20,38,55,56] (Table 2, see resonant structures of **3m**).

The emission properties of **3m–q** and Prodan evidenced that **3m** exhibits the maximum emission brightness ($\varepsilon \times \phi_F$) values with the following cases: **3m** 24 310 in dichloromethane (DCM) > **3q** 10 930 in acetonitrile (ACN) > **3p** 9200 in *N*,*N*-dimethylformamide (DMF) > Prodan 6560 in ACN > **3n** 3900 in acetone > **3o** 1320 in toluene (Tables 2, S22 and Fig. S42b). These results are consistent with the notable ICT process in **3m**, and the greater change of dipolar moment ($\Delta\mu$) value in its excited state with respect to the ground state ($\Delta\mu$ = 14.8 D), which was determined from Lippert–Mataga analysis[57] (Table 2 and Fig. S43, see SI for details). It is essential to note that a positive solvatofluorochromism behavior was observed in the emission data for the most polar dyes (*i.e.*, **3m**, **3p**, **3q**, and Prodan), in which the redshift is evident as the solvent polarity increases; however, **3n** and **3o** showed no trend in this property due to their lower polarity.[20,37] In addition, **3m** exhibited a higher fluorescence quantum yield (ϕ_F) in the solid state (ϕ_F = 90%) than **3m–q** and Prodan (ϕ_F of 23–64%); perhaps the superior intermolecular interaction of **3m** in the solid state, due to its high polarity, favors an increased aggregation-induced emission (AIE) process (Table 2, Fig. 2a and S44a).

The aggregation properties of **3m** in solution were evaluated by absorption and emission spectroscopy (see SI for details), and the results were consistent with those in the solid state. For example, upon additing water (up to 50% v/v) to **3m** in ACN, the absorption band at 344 nm decreased by up to 33% due to poor dye solubility in water (Fig. S44b). However, the emission band was redshifted (from 456 nm to 473 nm) as the water fraction increased (Fig. S44c), suggesting that water promotes the excimer formation[37,58] of **3m** *via* supramolecular interactions that induce aggregation in solution. Notably, emission bands in the aggregate state coincide in both the solution (λ_{em} = 472 nm, Fig. S44c) and the solid state (λ_{em} = 472 nm, Fig. 2a). Thus, the results for the aggregation of **3m** in solution validate our

Table 2 Summary of photophysical properties of **3m–q** and Prodan[a]

Fluorophore	λ_{abs}, λ_{em} (nm); range	ε, ϕ_F (%)	SS, $\Delta\mu$ (D)	LOD_F (μM), ϕ_F[b] (%)	Ref.
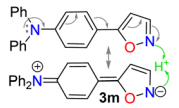	343–353, 406–458	44 780, 70 in DCM	115 in ACN, 14.80	$0.67^{turn\text{-}off}$ (456 nm), 90[b]	This work
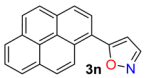	348–369, 394–404	18 820, 95 in acetone	60 in DMF, 4.67	$2.41^{turn\text{-}on}$ (350 nm), 23[b]	2025 (ref. 37)
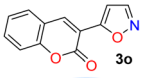	329–358, 402–416	16 220, 8 in toluene	79 in $CHCl_3$, 3.51	—, 64[b]	
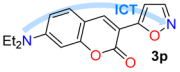	343–353, 406–458	36 080, 36 in DMF	63 in DMSO, 8.37	$3.38^{turn\ off}$ (482 nm), 49[b]	
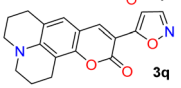	343–353, 406–458	53 600, 25 in ACN	49 in acetone, 5.75	$2.04^{turn\text{-}off}$ (498 nm), —	2025 (ref. 20)
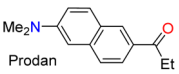	346–367, 418–502	14 080, 94 in ACN	135 in MeOH, 4.3 (ref. 59)	—, 35[b]	

[a] Experiments at 20 °C, a concentration of 27 μM, and using Prodan as a using Prodan as a standard. The average value of ε (in M^{-1} cm^{-1}), the highest value of ϕ_F, the highest value of Stokes Shifts (SS, λ_{em} − λ_{abs} in nm), the change of dipolar moment ($\Delta\mu$) value by Lippert–Mataga analysis, and limits of detection (LODs) for acidochromism (by TFA in ACN) are shown. [b] Data ϕ_F in the solid state are shown.

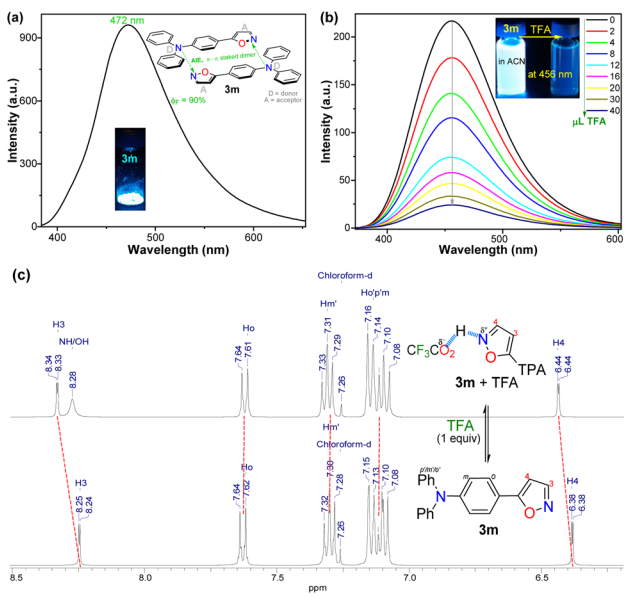

Fig. 2 Emission spectra of the fluorophore **3m** (a) in the solid state and (b) in MeCN with TFA (0–40 μL) at ~20 °C. Photographs taken under a 395 nm UV lamp are shown. (c) ^{1}H NMR spectra of **3m** upon the addition of TFA.

assumptions regarding its supramolecular interactions in the solid state.

To complete the photophysical analysis of **3m**, its acidochromism was studied by monitoring its absorption and emission spectra (at 27 μM in ACN) upon the addition of different amounts of TFA (0.1 M in ACN) to the probe (Table 2). Such as for **3n–q**,[20,37] it can be observed that changes in the absorption spectra are negligible and difficult to detect as the amount of TFA increases (Fig. S45a). Likewise, a noticeable change is observed in the emission spectra, with fluorescence turning off, exhibiting a limit of detection (LOD) of 0.67 μM (Fig. 2b and S45b). Although the binding mechanism of **3m–q** to TFA is similar and involves the azolic nitrogen atom (=N…H^+, established by ^{1}H NMR titration of **3n–q** in $CDCl_3$),[20,37] the new dye **3m** is the most sensitive probe (Table 2). The binding mechanism for **3m** was verified by ^{1}H NMR spectra in $CDCl_3$ with 1 equiv. of TFA, as this medium shifted the signals of the isoxazole ring (H3/H4, Fig. 2c and S46) to downfield, and the TPA moiety signals remained unchanged. Thus, the notable photophysics of **3m** in solution and in the solid state would favor its performance in chemosensors and materials science applications.

Finally, as none of the aminopyrazoles **4a–l** are fluorescent dyes, pyrazolopyrimidines **6a–c** were obtained using the MW-assisted reaction of **4′** or **4a,b** with 2,4-pentanedione (**5**),[43] to examine a synthetic application of **4a–l** (Scheme 6a) and the photophysics of **6a–c**. We have found that the 4-methoxyphenyl (4-anysyl) group favors the 7-(4-anysyl)-2-methylpyrazolo[1,5-*a*] pyrimidine (**6′**) fluorescence *via* ICT phenomena.[6,55,56] Thus, the photophysics of the 2-(4-anisyl) derivative **6c** was examined and compared with those of **6′**,[56] and the reference dyes **6a,b**, seeing that the variance in dihedral angles (DA) of **6c** and **6′** around their 4-anysyl group affects this property (Table S24 and Scheme 2b, see SI for more detail). The absorption and emission (Fig. S47) spectra of **6a–c** were measured in different-polarity solvents, showing **6c** a more intense ICT absorption band due to its 4-anysyl group. These dyes emit at ~440 nm without any

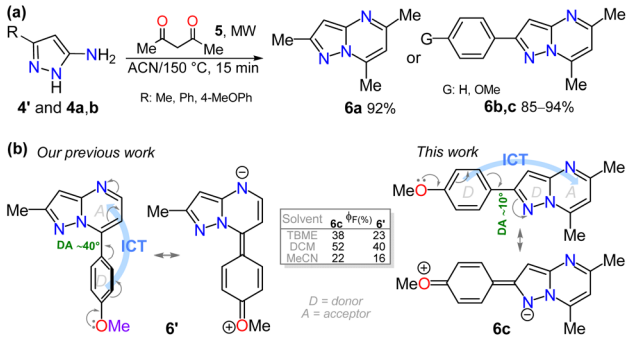

Scheme 6 (a) Synthesis of **6a–c** and (b) 4-anysyl substituted dyes **6′** and **6**.

solvatofluorochromic behavior, being **6b,c** more fluorescent (ϕ_F of 17–52%) than **6a** (ϕ_F = 4–17%).

The photophysical data of **6c** were also compared with those of **6′** under similar conditions[56] (Table S24 and Fig. S48), finding that most of the data were in the same range; however, **6c** displayed quantum yield values slightly higher (22–52%) than **6′** (16–40%),[56] perhaps due to the greater directionality in the ICT process of **6c**, slightly reduced by the electron-donor pyrazole moiety (Scheme 6b). Finally, TD-DFT calculations of electronic structure for **6a–c** and **6′** were conducted to further understand their photophysical properties. Studies were executed using ORCA 5.0.3,[60,61] with the B3LYP hybrid functional and the def2-TZVP/C basis set[62,63] due to the notable performance of this software on similar structures studied by us in this context[6,38,43,56] (Fig. S49; see SI for more details). This study validates that the dihedral angles in probes affect their electronic properties. Likewise, the energy gap values of these probes revealed that the presence of the 4-anisyl group in **6c** and **6′** reduces this energy by facilitating the ICT process; however, the presence of the 4-anisyl group at position 7 favors a better π-extended conjugation. Thus, the final studies revealed that **6b,c** and other analog compounds synthesized from 5-aminopyrazoles **4a–l** exhibit high photophysical potential.

Conclusions

In summary, a family of 5-(hetero)arylisoxazoles and of 5-amino-3-(hetero)aryl-NH-pyrazoles were synthesized under microwave conditions. Heteroamines were obtained using a TFA-catalyzed hydrazinolysis reaction, and both 1,2-azoles syntheses evidenced advantages against the other reported methods; *e.g.*, reduced reaction times, simple operation, good yields (52–95%), eco-compatibility (reactions in water), and using simpler and cheaper reagents – *e.g.*, β-anaminones used as starting materials were easily accessible from (hetero)aryl methyl ketones. However, the hydrazinolysis reaction does not work with isoxazoles bearing strongly electron-donating or electron-accepting groups, as these groups reduce the electrophilicity or basicity of the substrate, respectively. Moreover, the synthetic application of the obtained amines was developed to access pyrazolo[1,5-*a*]pyrimidine-based dyes; these dyes and the TPA-substituted isoxazole were photophysically studied, and results were compared with those of other reported analog dyes. The compounds described herein exhibited better photophysical properties than those of other reported fluorophores by us. Notably, mechanisms for accessing 5-aminopyrazoles *via* isoxazole ring-opening with hydrazine, and the photophysics of the pyrazolo[1,5-*a*]pyrimidine derivatives studied herein, were investigated using DFT calculations.

Experimental section

Comment. Structures of some relevant or novel intermediates and products were determined by NMR and HRMS (Fig. S3–S41). See SI for experimental procedures and characterization data for all compounds, including the general information. In addition, the SI contains information for the photophysics experiments.

Conflicts of interest

The authors declare no competing financial interest.

Author contributions

The individuals listed as authors have contributed to the development of this manuscript, and no other person was involved. The authors' contributions included: M.-C. R. and A. L.-B. developed experiments (synthesis and photophysical studies) and literature review, M.-C. R. and G. P. M. carried out the computational research (calculations, analysis, and writing), while J. P. developed and composed the original draft, supervised it, and provided sources. All authors have read and agreed to the published version of this manuscript.

Note added after first publication

This article replaces the version published on 11 February 2026 which contained errors in Table 2.

Data availability

The data supporting the findings of this search are available within the article and its supplementary information (SI). Supplementary information: supporting data for this article are provided in the SI, which includes experimental procedures and characterization data, HRMS analysis with spectra, NMR spectra, and computational and photophysical details. See DOI: https://doi.org/10.1039/d5ra09395c.

Acknowledgements

We thank the Chemistry Department and Vicerrectoría de Investigaciones (projects INV-2025-213-3467 and INV-2025-206-3289) of Universidad de Los Andes for financial support. We also recognize Sandra Ortiz and the High-Performance Computing (HPC) services for acquiring the mass spectra and for access to computational facilities.

Notes and references

1 A. Ansari, A. Ali and M. Asif, Shamsuzzaman, Review: biologically active pyrazole derivatives, *New J. Chem.*, 2016, **41**, 16–41.
2 S. Schenone, M. Radi, F. Musumeci, C. Brullo and M. Botta, Biologically driven synthesis of pyrazolo[3,4-d]pyrimidines as protein kinase inhibitors: An old scaffold as a new tool for medicinal chemistry and chemical biology studies, *Chem. Rev.*, 2014, **114**, 7189–7238.
3 G. J. Martis and S. L. Gaonkar, Advances in isoxazole chemistry and their role in drug discovery, *RSC Adv.*, 2025, **15**, 8213–8243.
4 Y. Shinde, B. Khairnar and S. Bangale, Exploring the Diverse Biological Frontiers of Isoxazole: A Comprehensive Review of its Pharmacological Significance, *ChemistrySelect*, 2024, **9**, e202401423.
5 N. N. Mallik, C. Manasa, V. Basavanna, D. C. Shanthakumar, S. Ningaiah and N. S. Lingegowda, Synthesis of Fused Isoxazoles: A Comprehensive Review, *Eng. Proc.*, 2023, **59**, 222.
6 J. Portilla, in *Advances in Heterocyclic Chemistry*, E. F. V. Scriven and C. A. Ramsden, Academic Press Inc. Elsevier, Amsterdam, Netherlands, 1st edn, 2024, vol. 142, pp. 71–138.
7 J. Portilla, Current Advances in Synthesis of Pyrazole Derivatives: An Approach Toward Energetic Materials, *J. Heterocycl. Chem.*, 2024, **61**, 2026–2039.
8 Y. Wang, C. Xiong, J. Zhong and Q. Zhou, Synthesis of 1,3,5-trisubstituted pyrazole-4-carboxylates through 1,3-dipolar cycloaddition of nitrilimines with allenoates, *Tetrahedron*, 2022, **115**, 132790.
9 P. K. Mykhailiuk, Fluorinated Pyrazoles: From Synthesis to Applications, *Chem. Rev.*, 2021, **121**, 1670–1715.
10 M. Nidhar, S. Khanam, P. Sonker and P. Gupta, Bioorganic Chemistry Click inspired novel pyrazole-triazole-persulfonimide & pyrazole-triazole-aryl derivatives ; Design , synthesis , DPP-4 inhibitor with potential anti-diabetic agents, *Bioorg. Chem.*, 2022, **120**, 105586.
11 A. H. H. Ahmed, M. F. A. Mohamed, R. M. Allam, A. Nafady, S. K. Mohamed, A. E. Gouda and E. A. M. Beshr, Design, synthesis, and molecular docking of novel pyrazole-chalcone analogs of lonazolac as 5-LOX, iNOS and tubulin polymerization inhibitors with potential anticancer and anti-inflammatory activities, *Bioorg. Chem.*, 2022, **129**, 106171.
12 A. V Galenko, A. F. Khlebnikov, M. S. Novikov, V. V Pakalnis and N. V Rostovskii, Recent advances in isoxazole chemistry, *Russ. Chem. Rev.*, 2015, **84**, 335–377.
13 J. Zhu, J. Mo, H. Lin, Y. Chen and H. Sun, The recent progress of isoxazole in medicinal chemistry, *Bioorg. Med. Chem.*, 2018, **26**, 3065–3075.
14 K. Ghosh, N. Nayek, S. Das, N. Biswas and S. Sinha, Design and synthesis of ferrocene-tethered pyrazolines and pyrazoles: Photophysical studies, protein-binding behavior with bovine serum albumin, and antiproliferative activity against MDA-MB-231 triple negative breast cancer cells, *Appl. Organomet. Chem.*, 2021, **35**, 1–10.
15 R. Verma, S. K. Verma, K. P. Rakesh, Y. R. Girish, M. Ashrafizadeh, K. S. Sharath Kumar and K. S. Rangappa, Pyrazole-based analogs as potential antibacterial agents against methicillin-resistance staphylococcus aureus (MRSA) and its SAR elucidation, *Eur. J. Med. Chem.*, 2021, **212**, 113134.
16 A. Restrepo-Acevedo, N. Osorio, L. E. Giraldo-López, R. F. D'Vries, S. Zacchino, R. Abonia, R. Le Lagadec and F. Cuenú-Cabezas, Synthesis and antifungal activity of nitrophenyl-pyrazole substituted Schiff bases, *J. Mol. Struct.*, 2022, **1253**, 132289.
17 M. F. Harras, R. Sabour and O. M. Alkamali, Discovery of new non-acidic lonazolac analogues with COX-2 selectivity as potent anti-inflammatory agents, *MedChemComm*, 2019, **10**, 1775–1788.
18 N. Gajraj, COX-2 Inhibitors Celecoxib and Parecoxib: Valuable Options for Postoperative Pain Management, *Curr. Med. Chem.*, 2007, **7**, 235–249.
19 M. Moiola, A. Bova, S. Crespi, M. G. Memeo, M. Mella, H. S. Overkleeft, B. I. Florea and P. Quadrelli, Fluorescent Probes from Aromatic Polycyclic Nitrile Oxides: Isoxazoles versus Dihydro-1λ3,2λ4-Oxazaborinines, *ChemistryOpen*, 2019, **8**, 770–780.
20 M.-C. Ríos, N.-F. Bravo, M. Macías, B. A. Iglesias and J. Portilla, Synthesis and Photophysical Study of 3-(Isoxazol-5-yl)coumarins, *ChemPhotoChem*, 2025, **9**, e202400389.
21 N. E. Astakhova, K. S. Sadovnikov, D. A. Vasilenko, A. A. Markova, M. T. Nguyen, I. D. Burtsev, A. A. Yakushev, Y. K. Grishin, Y. A. Gracheva, Y. L. Volodina, A. R. Lukmanova, V. V. Spiridonov, A. A. Yaroslavov, A. D. Averin, V. A. Kuzmin, E. R. Milaeva and E. B. Averina, Isoxazole-based styryl dyes with macrocyclic receptors: synthesis, ion sensing properties and applications in bioimaging, *J. Photochem. Photobiol., A*, 2025, **468**, 116497.
22 P. Yin, L. A. Mitchell, D. A. Parrish and J. M. Shreeve, Comparative Study of Various Pyrazole-based Anions: A Promising Family of Ionic Derivatives as Insensitive Energetic Materials, *Chem.–Asian J.*, 2017, **12**, 378–384.
23 P. E. Guzmán, R. C. Sausa, L. A. Wingard, R. A. Pesce-Rodriguez and J. J. Sabatini, Synthesis and Characterization of Isoxazole-Based Energetic Plasticizer Candidates EEIN and IDN, *Eur. J. Org Chem.*, 2018, **2018**, 6724–6728.
24 A. Ghaedi, G. R. Bardajee, A. Mirshokrayi, M. Mahdavi, A. Shafiee and T. Akbarzadeh, Facile, novel and efficient synthesis of new pyrazolo[3,4-b]pyridine products from condensation of pyrazole-5-amine derivatives and activated carbonyl groups, *RSC Adv.*, 2015, **5**, 89652–89658.
25 H. A. Abdel-Aziz, T. S. Saleh and H. S. A. El-Zahabi, Facile Synthesis and In-Vitro Antitumor Activity of Some Pyrazolo[3,4-b]pyridines and Pyrazolo[1,5-a]pyrimidines Linked to a Thiazolo[3,2-a]benzimidazole Moiety, *Arch. Pharm.*, 2010, **343**, 24–30.

26 J. H. Sahner, M. Groh, M. Negri, J. Haupenthal and R. W. Hartmann, Novel small molecule inhibitors targeting the "switch region" of bacterial RNAP: Structure-based optimization of a virtual screening hit, *Eur. J. Med. Chem.*, 2013, **65**, 223–231.
27 F. Bell, 51. 5-Amino-1-aryl-3-methylpyrazoles, *J. Chem. Soc.*, 1941, 285–287.
28 A. M. Jawalekar, E. Reubsaet, F. P. J. T. Rutjes and F. L. van Delft, Synthesis of isoxazoles by hypervalent iodine-induced cycloaddition of nitrile oxides to alkynes, *Chem. Comm.*, 2011, **47**, 3198–3200.
29 S. Das and K. Chanda, An overview of metal-free synthetic routes to isoxazoles: the privileged scaffold, *RSC Adv.*, 2021, **11**, 32680–32705.
30 N. Kallman, K. Cole, T. Koenig, J. Buser, A. McFarland, L. McNulty and D. Mitchell, Synthesis of Aminopyrazoles from Isoxazoles: Comparison of Preparative Methods by in situ NMR Analysis, *Synthesis*, 2016, **48**, 3537–3543.
31 W. Seelen, M. Schäfer and A. Ernst, Selective ring N-protection of aminopyrazoles, *Tetrahedron Lett.*, 2003, **44**, 4491–4493.
32 A. Katritzky, A. Vakulenko, J. Sivapackiam, B. Draghici and R. Damavarapu, Synthesis of Dinitro-Substituted Furans, Thiophenes, and Azoles, *Synthesis*, 2008, **2008**, 699–706.
33 P. J. Gilligan, T. Clarke, L. He, S. Lelas, Y.-W. Li, K. Heman, L. Fitzgerald, K. Miller, G. Zhang, A. Marshall, C. Krause, J. F. McElroy, K. Ward, K. Zeller, H. Wong, S. Bai, J. Saye, S. Grossman, R. Zaczek, S. P. Arneric, P. Hartig, D. Robertson and G. Trainor, Synthesis and Structure–Activity Relationships of 8-(Pyrid-3-yl)pyrazolo[1,5- *a*]-1,3,5-triazines: Potent, Orally Bioavailable Corticotropin Releasing Factor Receptor-1 (CRF 1)Antagonists, *J. Med. Chem.*, 2009, **52**, 3084–3092.
34 D. Mitchell, Y. Luo, L. McNulty, J. Buser and A. McFarland, A Convenient and Practical Synthesis of Aminopyrazoles, *Synthesis*, 2015, **47**, 235–241.
35 M. P. Ponda, J. L. Breslow, H. Selnick, and M. Egbertson, Aminoacylindazole immunomodulators for treatment of autoimmune diseases, *WO Pat.*, WO2017205296A1, 2017.
36 A. B. Inkerton, S. T. Meyer, and R. J. Elsdon, Pyridine checkpoint kinase 1 (CHK1) inhibitors and uses thereof, *WO Pat.*, WO2023230477A1, 2023.
37 M.-C. Ríos, A. Ladino-Bejarano and J. Portilla, Synthesis and Photophysics of 5-(1-Pyrenyl)-1,2-Azoles, *Chemistry*, 2025, **7**, 120.
38 A. Tigreros, S.-L. Aranzazu, M.-C. Ríos and J. Portilla, Pyrazolo[1,5-a]pyrimidine–Dioxaborinine Hybrid Dyes: Synthesis and Substituent Effect in the Photophysical Properties, *Eur. J. Org Chem.*, 2023, **2023**, e202300089.
39 P. G. Rao, B. Saritha and T. S. Rao, Highly selective reaction based colorimetric and fluorometric chemosensors for cyanide detection via ICT off in aqueous solution, *J. Photochem. Photobiol., A*, 2019, **372**, 177–185.
40 M. J. Peng, Y. Guo, X. F. Yang, F. Suzenet, J. Li, C. W. Li and Y. W. Duan, Coumarin-hemicyanine conjugates as novel reaction-based sensors for cyanide detection: Convenient synthesis and ICT mechanism, *RSC Adv.*, 2014, **4**, 19077–19085.
41 S. Erdemir and S. Malkondu, Cyanobiphenyl-spiropyrane and -hemicyanine conjugates for cyanide detection in organic/aqueous media through reverse ICT direction: Their practical applications, *Talanta*, 2021, **231**, 122385.
42 Z. Huang, L. Li, Y. Zhao, H. Wang and D. Shi, An Efficient Synthesis of Isoxazoles and Pyrazoles under Ultrasound Irradiation, *J. Heterocycl. Chem.*, 2014, **51**, E309–E313.
43 S. L. Aranzazu, A. Tigreros, A. Arias-Gómez, J. Zapata-Rivera and J. Portilla, BF3-Mediated Acetylation of Pyrazolo[1,5-a] pyrimidines and Other π-Excedent (N-Hetero)arenes, *J. Org. Chem.*, 2022, **87**, 9839–9850.
44 C. Cifuentes, N. Bravo, D. Restrepo, M. Macías and J. Portilla, Isomerization of pirazolopyrimidines to pyrazolopyridines by ring-opening/closing reaction in aqueous NaOH, *RSC Adv.*, 2025, **15**, 2078–2085.
45 M. M. Ghorab, M. S. Alsaid, G. H. Al-Ansary, G. A. Abdel-Latif and D. A. Abou El Ella, Analogue based drug design, synthesis, molecular docking and anticancer evaluation of novel chromene sulfonamide hybrids as aromatase inhibitors and apoptosis enhancers, *Eur. J. Med. Chem.*, 2016, **124**, 946–958.
46 H. O. Tawfik, M. A. Shaldam, A. Nocentini, R. Salem, H. Almahli, S. T. Al-Rashood, C. T. Supuran and W. M. Eldehna, Novel 3-(6-methylpyridin-2-yl)coumarin-based chalcones as selective inhibitors of cancer-related carbonic anhydrases IX and XII endowed with anti-proliferative activity, *J. Enzyme Inhib. Med. Chem.*, 2022, **37**, 1043–1052.
47 F. A. Rosa, P. Machado, H. G. Bonacorso, N. Zanatta and M. A. P. Martins, Reaction of β-dimethylaminovinyl ketones with hydroxylamine: A simple and useful method for synthesis of 3- and 5-substituted isoxazoles, *J. Heterocycl. Chem.*, 2008, **45**, 879–885.
48 R. J. RamaRao, A. K. S. B. Rao, N. Sreenivas, B. S. Kumar and Y. L. N. Murthy, Synthesis and Antibacterial Activity of Novel 5-(heteroaryl)isoxazole Derivatives, *J. Korean Chem. Soc.*, 2011, **55**, 243–250.
49 M. J. Frisch, G. W. Trucks, H. B. Schlegel, G. E. Scuseria, M. A. Robb, J. R. Cheeseman, G. Scalmani, V. Barone, G. A. Petersson, H. Nakatsuji, X. Li, A. V. Marenich, A. V. Marenich, J. Bloino, B. G. Janesko, R. Gomperts, B. Mennucci, H. P. Hratchian, J. V. Ortiz, A. F. Izmaylov, J. L. Sonnenberg, D. Williams-Young, F. Ding, F. Lipparini, F. Egidi, J. Goings, B. Peng, A. Petrone, T. Henderson, D. Ranasinghe, V. G. Zakrzewski, J. Gao, N. Rega, G. Zheng, W. Liang, M. Hada, M. Ehara, K. Toyota, R. Fukuda, J. Hasegawa, M. Ishida, Y. Nakajima, Y. Honda, O. Kitao, H. Nakai, T. Vreven, K. Throssell Jr. J. A. Montgomery, J. E. Peralta, F. Ogliaro, M. J. Bearpark, J. J. Heyd, E. N. Brothers, K. N. Kudin, V. N. Staroverov, T. A. Keith, R. Kobayashi, J. Normand, K. Raghavachari, A. P. Rendell, J. C. Burant, S. S. Iyengar, J. Tomasi, M. Cossi, J. M. Millam, M. Klene, C. Adamo, R. Cammi, J. W. Ochterski, R. L. Martin, K. Morokuma, O. Farkas, J. B. Foresman and D. J. Fox, *Gaussian 16, Revision C.01*, Gaussian, Inc., 2016.
50 Y. Zhao and D. G. Truhlar, Exploring the Limit of Accuracy of the Global Hybrid Meta Density Functional for Main-Group

Thermochemistry, Kinetics, and Noncovalent Interactions, *J. Chem. Theory Comput.*, 2008, **4**, 1849–1868.

51 Y. Zhao and D. G. Truhlar, Applications and validations of the Minnesota density functionals, *Chem. Phys. Lett.*, 2011, **502**, 1–13.

52 N. Mardirossian and M. Head-Gordon, How Accurate Are the Minnesota Density Functionals for Noncovalent Interactions, Isomerization Energies, Thermochemistry, and Barrier Heights Involving Molecules Composed of Main-Group Elements?, *J. Chem. Theory Comput.*, 2016, **12**, 4303–4325.

53 N. Q. Trung, A. Mechler, N. T. Hoa and Q. V. Vo, Calculating bond dissociation energies of X–H (X=C, N, O, S) bonds of aromatic systems via density functional theory: a detailed comparison of methods, *R. Soc. Open Sci.*, 2023, **9**, 220177.

54 N. R. Elejalde-Cadena, M. García-Olave, D. Figueroa, P. Vidossich, G. Pietro Miscione and J. Portilla, Influence of Steric Effect on the Pseudo-Multicomponent Synthesis of N-Aroylmethyl-4-Arylimidazoles, *Molecules*, 2022, **27**, 1165.

55 A. Tigreros, J. C. Castillo and J. Portilla, Cyanide chemosensors based on 3-dicyanovinylpyrazolo[1,5-a] pyrimidines: Effects of peripheral 4-anisyl group substitution on the photophysical properties, *Talanta*, 2020, **215**, 120905.

56 A. Tigreros, S.-L. Aranzazu, N.-F. Bravo, J. Zapata-Rivera and J. Portilla, Pyrazolo[1,5-a]pyrimidines based fluorophores: A comprehensive theoretical-experimental study, *RSC Adv.*, 2020, **10**, 39542–39552.

57 U. Subuddhi, S. Haldar, S. Sankararaman and A. K. Mishra, Photophysical behaviour of 1-(4-N,N-dimethylaminophenylethynyl)pyrene (DMAPEPy) in homogeneous media, *Photochem. Photobiol. Sci.*, 2006, **5**, 459–466.

58 A. J. Musser, S. K. Rajendran, K. Georgiou, L. Gai, R. T. Grant, Z. Shen, M. Cavazzini, A. Ruseckas, G. A. Turnbull, I. D. W. Samuel, J. Clark and D. G. Lidzey, Intermolecular states in organic dye dispersions: excimers vs. aggregates, *J. Mater. Chem. C*, 2017, **5**, 8380–8389.

59 A. Kawski, Ground-and Excited-State Dipole Moments of 6-Propionyl-2-(dimethylamino)naphthalene Determined from Solvatochromic Shifts, *Z. Naturforsch. A*, 1999, **54**, 379–381.

60 F. Neese, Software update: The ORCA program system, version 5.0, *Wiley Interdiscip. Rev. Comput. Mol. Sci.*, 2022, **12**(5), e1606.

61 F. Neese, The ORCA program system, *Wiley Interdiscip. Rev. Comput. Mol. Sci.*, 2012, **2**, 73–78.

62 F. Neese, F. Wennmohs, U. Becker and C. Riplinger, The ORCA quantum chemistry program package, *J. Chem. Phys.*, 2020, **152**(22), 224108.

63 V. Barone and M. Cossi, Quantum Calculation of Molecular Energies and Energy Gradients in Solution by a Conductor Solvent Model, *J. Phys. Chem. A*, 1998, **102**, 1995–2001.